

THE INFLUENCE OF SIMULATED THERMAL CYCLE ON THE FORMATION OF MICROSTRUCTURES OF MULTI-PASS WELD METAL

Received - Priljeno: 2004-03-20

Accepted - Prihvaeno: 2004-07-10

Original Scientific Paper - Izvorni znanstveni rad

In the present work was analysed the influence of weld thermal cycle on the microstructural changes in weld metal by use of the simulated microstructures. We examined the kinetics of the formation of austenite from the starting microstructure. The simulated microstructures were prepared by the application of simulated thermal cycles with different peak temperatures on a sample of real single-pass weld metal. The reproduction of thermal cycles were carried out by the SMITWELD simulator. Special attention was dedicated to the influence of thermal cycle on the formation of microstructures, which can be potential triggers of brittle fracture (local brittle zones).

Key words: *weld joint, multi-pass weld metal, simulated microstructure, impact toughness*

Utjecaj simuliranog termičkog ciklusa na stvaranje mikrostruktura višeprolaznog zavar. U ovom radu je eksperimentalno analiziran utjecaj termičkog ciklusa kod zavarivanja na mikrostrukturne promjene u zavaru. Simulirane mikrostrukture bile su pripremljene pri termičkim ciklusima različitih maksimalnih temperatura na uzorcima realnog jedno prolaznog zavar. Simulirani termički ciklusi bili su izvedeni na SMITWELD simulatoru termičkog ciklusa. Posebna pažnja bila je usmjerena utjecaju termičkog ciklusa na stvaranje mikrostruktura, koje bi mogle biti potencijalna mjesta za krti lom (lokalno krte zone).

Ključne riječi: *zavareni spoj, višeprolazni zavar, simulirana mikrostruktura, udarna žilavost*

INTRODUCTION

The metallurgical heterogeneity influences on the fracture behaviour of weld joint [1, 2]. The parameters which influence on the initiation, propagation and arresting the crack respectively fracture in weld joint can be divided into three group: the geometry of weld joint (a), the presence of residual stresses (b) and the metallurgical heterogeneity of weld joint (c) [3, 4]. The combination of the mentioned parameters can cause the unstable fracture and the difficulty at the evaluation of experimental results, too [1, 5].

The thermal cycles at the multi-pass welding increase the heterogeneity of the mechanical and the metallurgical properties of weld joint [6, 7]. They can cause the formation of local brittle zones (LBZ), which are frequently the trigger of brittle fracture [8 - 10]. The fracture initiation at the crack tip depends on: the geometry of specimen (a), the mechanical properties of material at the crack tip (b) and the temperature (c) [11, 12]. The interaction between the heterogeneous microstructures, which are particularly significantly for the multi-pass weld joint, can cause

the fracture of weld joint at relatively low deformations. The LBZ can strongly influence on the toughness of weld joint [7, 14].

The resistance of weld metal against the brittle fracture depends from the finally microstructure. The proportion between the ferrite at the austenite grain boundaries (boundary nucleation) and the ferrite inside of the austenite grain (intergranular nucleation), and the concentration of alloy elements (Al, Si, Ti, B, Nb, Mo) strongly influence on the toughness of weld metal [15]. It is generally recognized that the existence of components with very low toughness (martensite-austenite constituent) and the segregation of impurities in weld metal seriously reduce the toughness of weld joint [16]. The optimal concentration of carbides can hinder the growth of primary austenite grains and can create the additional conditions for the formation of microstructure with good strength and toughness.

In the present work was experimentally analysed the influence of weld thermal cycle on the microstructural changes in the weld metal. The kinetics of the formation of austenite from the starting microstructure was examined. Special attention was dedicated to the influence of weld thermal cycle on the formation of microstructures, which can be potential triggers of brittle fracture (LBZ).

D. Rojko, V. Gliha, Faculty of Mechanical Engineering University of Maribor, Maribor, Slovenia

EXPERIMENTAL PROCEDURES

Preparing the samples for the experimental work

As base for the experimental work was used a real single-pass weld metal. The real single-pass weld metal was produced by the submerge arc welding (SAW). The welding groove has the "V" shape. It was manufactured on the steel plate NIOMOL 490K (Figure 1.).

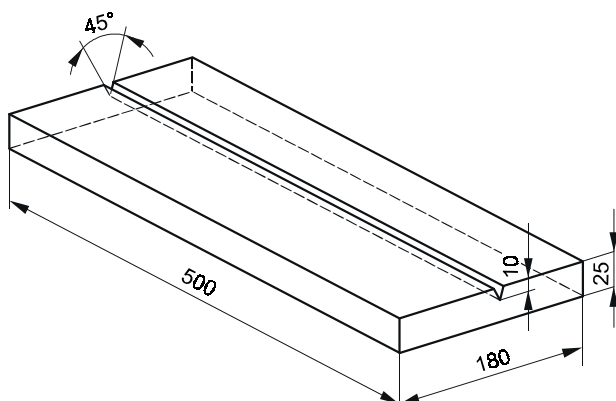


Figure 1. Shape and dimensions of welding plate
Slika 1. Oblik i dimenzije zavarivane ploče

The real single-pass weld metal was produced by tubular wire FILTUB 128 and welding flux FBTT. The average input energy was $Q = 21$ kJ/cm. The preheating tem-

Table 1. Chemical composition of weld metal
Tablica 1. Kemijski sastav zavara

Chemical element mass. / %	C	Si	Mn	Mo	Ni
FILTUB 128	0,05	0,20	1,40	0,40	1,20

perature was $T_{\text{preh.}} = 40$ °C and the experimental cooling times $\Delta t_{8/5}$ were between 12,6 s and 13,2 s. The chemical composition and the mechanical properties of weld metal are shown in Tables 1. and 2.

Table 2. Mechanical properties of weld metal
Tablica 2. Mehanička svojstva zavara

	$R_{p0,2}$ / MPa	R_m / MPa	A_5 / %	$A_v(-60$ °C) / J
FILTUB 128	> 550	630 - 730	> 20	280, 271, 294

The researches of the mechanical properties and the metallographic examinations were performed on the real single-pass weld metal and on simulated microstructures of double-pass weld metal. The simulated microstructures were prepared by the application of the single thermal cycle with different peak temperatures on the samples of the real single-pass weld metal. The samples of the real single-

pass weld metal with dimension $9 \times 9 \times 55$ mm were cut out from V-shaped single-pass welded joint (Figure 2.).

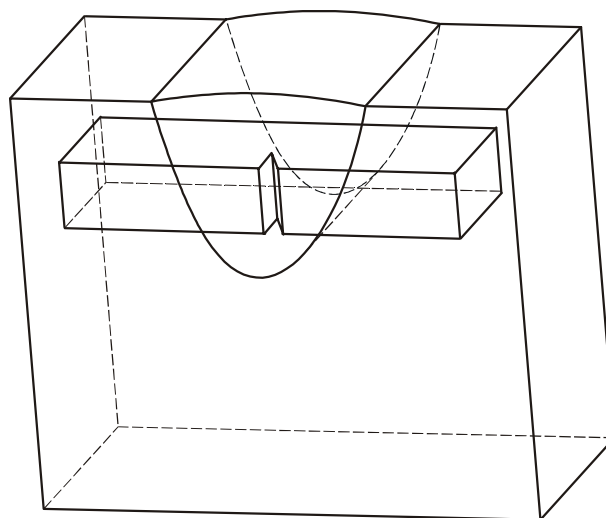


Figure 2. Cutting the sample for simulation from the V-shaped single-pass welded joint and the position of mechanical notch of Charpy specimen

Slika 2. Uzorak za simulaciju iz jednoprolaznog zavarivane spoja sa V-oblikom i pozicija mehaničkog zarez na Charpy uzorku

The impact toughness measurements of the real single-pass weld metal and the simulated microstructures were carried out by the Charpy specimens with dimension $8 \times 8 \times 55$ mm. The Charpy specimens were cut out from V-shaped single-pass weld joint respectively they were manufactured from the samples of simulated microstructures. The mechanical notch was located in the middle of the specimen length in the direction of thickness of the single-pass weld joint (Figure 2.). It was 2 mm deep. From the simulated microstructures were also prepared the samples for the measurements of concentration of retained austenite and carbides in weld metal by the X-ray diffraction.

Form the simulated microstructures of two-pass weld metal

It is useful to be simulate the weld thermal cycle under laboratory conditions in order to obtain information about microstructural and property changes in the HAZ and in the weld metal. Although, in principle, these changes can be observed and measured from real welds, in practice it is more convenient to work with test pieces representative of one, not a range, of microstructures and grain size, particularly if mechanical property measurement are required.

The simulated microstructures were prepared by the application of thermal cycles with different peak temperatures (T_p) on the samples of the real single-pass weld metal. The real single-pass weld metal was the base for analysis the properties of first-pass. The reproduction of thermal

cycles were performed by the SMITWELD simulator. The thermal cycle was programmed by the welding heat-flow theory. The mathematical model for two-dimensional heat flow (Rykalin equations) was used. The parameters for programming the welding thermal cycle were: thermal characteristics of weld metal (a), starting temperature of sample (b), heating rate (c), peak temperature of thermal cycle (d) and cooling time $\Delta t_{8/5}$ (e). For the thermal characteristics of weld metal were used already known thermal characteristics of micro alloying steel.

The samples were heated by electro-resistance. They were fixed between the two water-cooling metal clamps. The clamps were conducted AC current with voltage about 50 V. The maximum temperature was generate in the middle of the sample, where was placed the thermocouple Pt/PtRh, too. The phase transformations were analysed by a dilatometer. The dilatometer was fixed in the region of maximum temperature accordingly in the middle of the sample. It has measured the variation of cross-section during the acting of thermal cycle. During the simulation, the clamps and the dilatometer were located in a shielding chamber, which was filled up by shielding gas Ar.

The simulated microstructures of double-pass weld metal were prepared by the application of single thermal cycles with four different peak temperatures ($T_p = 780, 980, 1100, 1350$ °C) on the samples of the real single-pass weld metal. The real single-pass weld metal was heated to the different peak temperatures (T_p) by the heating rate 200 K/s. After the short keeping time at peak temperature (3 s), the samples were cooled to the room temperature accordingly in the middle of the sample. When the peak temperature (T_p) was lower since 800 °C, the cooling time $\Delta t_{8/5}$ was defined by relation $\Delta t_{5/3} \cong 2 \Delta t_{8/5}$ [17]. The simulation parameters are shown in Table 3.

Table 3. Simulation parameters of double-pass weld metal
 Tablica 3. Simulacijski parametri dvoprolaznog zavrata

Sample	Peak temperature T_p / °C	$\Delta t_{8/5}$ / s	$\Delta t_{5/3} \cong 2 \Delta t_{8/5}$ / s
SM1*			
SM2	780		25,8 – 26,2
SM3	980	13,1 – 13,3	
SM4	1100	12,7 – 12,9	
SM5	1350	12,5 – 12,8	

* – real single - pass weld metal

RESULTS AND DISCUSSION

The impact toughnesses of the real single-pass weld metal and of the simulated microstructures of double-pass weld metal were determined by the Charpy specimens with dimensions 8×8×55 mm at – 30 °C. Those results of impact

toughness were corrected by a correcting polynom [18]. The correcting polynom has taken into the consideration the difference between the impact energy of generally size of Charpy specimen (dimension 10×10×55 mm) and the im-

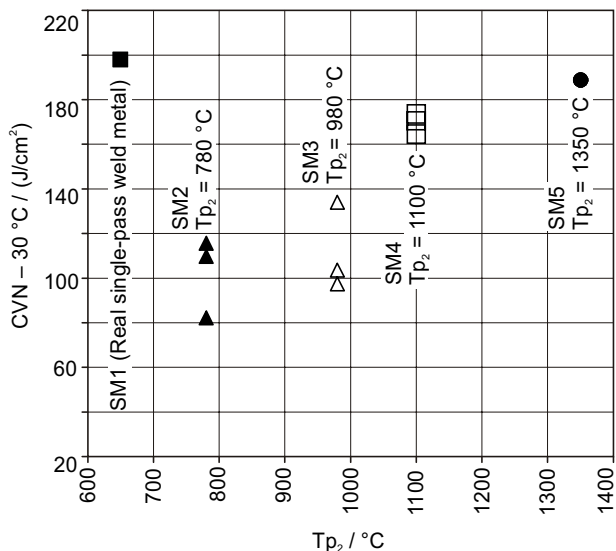


Figure 3. The results of impact toughness
 Slika 3. Rezultati ispitivanja udarne žilavosti

pact energy of Charpy specimen with dimensions 8×8×55 mm. The results of impact toughness are shown in Figure 3., meanwhile the concentration of retained austenite and carbides in simulated microstructures are shown in Table 4.

Table 4. Concentration of retained austenite and carbides in simulated microstructures
 Tablica 4. Koncentracija zaostalog austenita i karbida u simuliranim mikrostrukturama

	SM2	SM3
Retained austenite / vol. %	1,9	3,9
Carbides / vol. %	< 4.0	

The largest toughness has the microstructure of the real single-pass weld metal SM1 (Figure 3.). Polygonal ferrite (PF) has formed in the grain boundaries of the prior austenite, but not in sufficient quantity to form a network or veining. The acicular ferrite (AF) is much coarser because of the slower cooling $\Delta t_{8/5} \approx 13$ s. The microstructure of the real single-pass weld metal was composed also of ferrite aligned with secondary phases (AC) This constituents develops when the proeutectoid ferrite nucleates in the austenite grain boundaries at the start of transformation and grows as lamellar-like plates toward the interior of the austenite grains. Very small amounts of martensite and austenite as minute grains can be retained between the ferrite side plates, too (Figure 4.).

The simulated microstructure of double-pass weld metal SM2 was heated to the temperature range between A_{c1} and

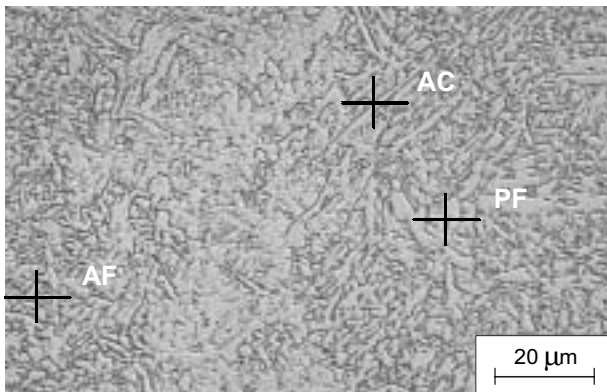


Figure 4. Microstructure of real single-pass weld metal composed of polygonal ferrite (PF), ferrite with aligned secondary phase (AC) and acicular ferrite (AF)

Slika 4. Mikrostruktura realnog jednoproložnog zavara koji se sastoji iz poligonalnog ferita (PF) i acikularnog ferita (AF)

A_{c_3} . High heating rate of 200 K/s to the relatively low peak temperature ($T_{p_2} = 780\text{ °C}$) has caused the formation of austenite with carbon inhomogeneities and residual carbides. During the heating to the peak temperature the areas of high-carbon austenite, formed from bainite microstructure of the real single-pass weld metal, have not been given time for carbon to diffuse into grains of low carbon austenite that are just starting to form. Superheating (short heating time) and presence of carbides (< 4 vol. %) have affected on the extent of the α - γ phase transformation. In the regions of high-carbon austenite the γ - α phase transformation has started at lower temperature. The high-carbon austenite, upon cooling to the room temperature has produced a harder microstructure that also had low toughness (Figure 5.).

The share and hardness of harder microstructure were depended upon the carbon concentration and cooling rate. The high-carbon austenite had under cooled and then transformed to the martensite. The rest of austenite (retained austenite) has remained untransformed (1,9 vol. %). The austenite-martensite constituents (M-A constituents) on the grain boundaries (Figure 5.) have influenced on the impact toughness, which was the lowest in compare with the rests of the simulated microstructures.

Detection of the small amounts of retained austenite in weld metal often requires precisely metalographic examination. High magnification and special etching technique may be required if the austenite is present as small areas. Figure 6. illustrates the microstructure of sample SM3 ($T_{p_2} = 980\text{ °C}$) which was etched with picral solution (four percent picric acid in ethyl alcohol). As we see, the presence of considerable retained austenite (3,9 vol. %) and martensite is revealed.

The high peak temperature has caused the austenitization of weld metal, but the austenite had carbon inhomogeneities and residual carbides. The areas of high-carbon austenite formed from bainite microstructure have been

given time for carbon to diffuse into grains of low carbon austenite that are just starting to form. During the transformation mechanism γ - α , carbon diffused from the acicular ferrite regions into the remaining austenite. The retention of some austenite in the final simulated microstructure of double-pass weld metal SM3 was the consequence of enrichment of austenite with carbon adjacent to the interface with the ferrite. Additional reason for small regions of austenite to remain untransformed were also the compressive stresses imposed by the surrounding acicular ferrite. The

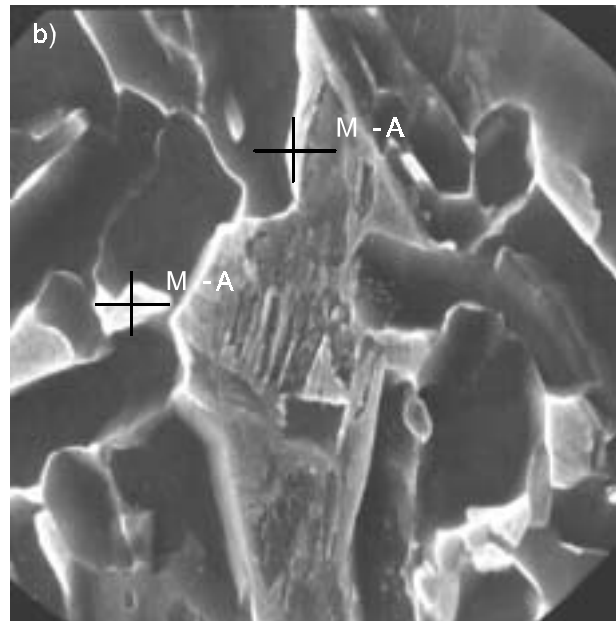
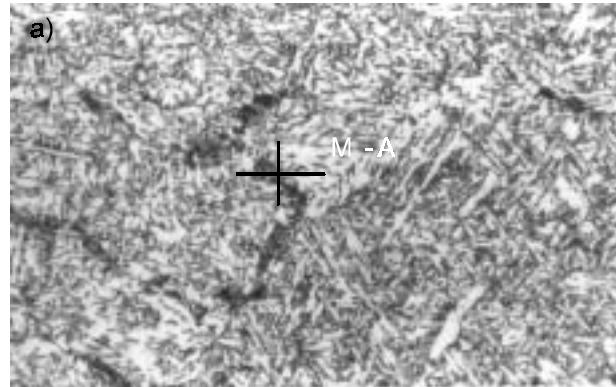


Figure 5. Simulated microstructure of double-pass weld metal, ($T_{p_2} = 780\text{ °C}$):

a) Intercritical heated region of weld metal with M-A constituents on the grain boundaries, original magnification: 500 \times ,
b) M-A constituents on the grain boundaries, SEM, original magnification: 10 000 \times

Slika 5. Simulirana mikrostruktura dvoproložnog zavara, ($T_{p_2} = 780\text{ °C}$):

a) Interkritičko zagrijano područje zavara sa M-A konstituentima, na granicama zrna, izvorno povećanje 500 \times ,
b) M-A konstituenti, na granicama zrna, SEM, izvorno povećanje 10 000 \times

small share of high-carbon austenite, upon cooling to the room temperature, transformed to martensite, which has influenced markedly on the decreasing of impact toughness. Because of superheating the dissolution of carbides has occurred at temperatures much greater than expected solubility temperature. Presence of carbides have affected on the extent of the α - γ phase transformation and grain growth. Small concentration of carbides has limited the potential nucleation sites for the formation of austenite and it extend time for austenitization. The existential nucleation sites have saturated rapidly, however the new nucleation sites have not appeared in sufficient quantity. Martensite is likely to

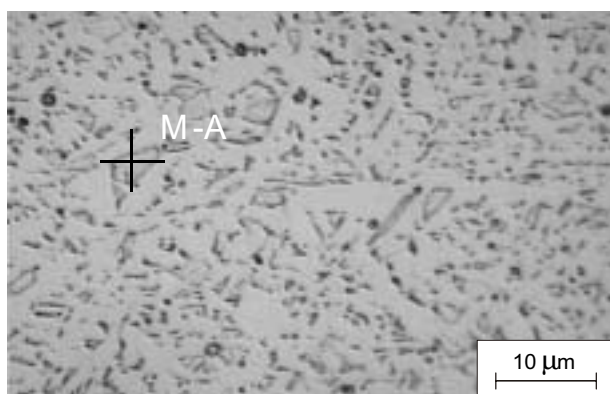


Figure 6. **Simulated microstructure of martensite (M) and retained austenite (A) ($T_{p_2} = 980\text{ °C}$)**

Slika 6. **Simulirana mikrostruktura martenzita (M) i zaostalog austenita (A) ($T_{p_2} = 980\text{ °C}$)**

be quite brittle, and retained austenite can be unstable. The retained microphases have existed in the simulated microstructure of double-pass weld metal SM3 as isolated islands. They were located in the interior of the primary crystal grains. Fast cooling rate has facilitated retention of the austenite and the martensite. Several alloying elements (Nb, Mo, Al) have promoted the hardenability. They caused the formation of the micro-segregation. Although the short time was available during the weld thermal cycle, carbon was time for diffusing from the austenite, that was undergoing austenite to ferrite transformation, to the martensite and retained austenite. The concentration of carbon in the martensite and in the retained austenite was increased. During the impact test, those brittle microphases have acted as the cleavage fracture initiators (Figure 7.). They assisted for the easily initiation of cleavage fracture and also for faster propagation of fracture. The initiation and the propagation of brittle fracture have appeared as consequence of the slide of dislocations in the ferrite matrix ahead of M-A constituents and as consequence of the plastic deformation in the small region at the crack tip.

High heating rate and high temperature of simulation cycle ($T_{p_2} = 1100\text{ °C}$) have caused the partial dissolution of carbides (presumably cementite) and they have limited grain

growth. The undissolved carbides have impeded the excessive growth of austenite grain. As the probability of γ - α phase transformation is proportionally with the largeness of the austenite grain boundaries, the γ - α phase transforma-

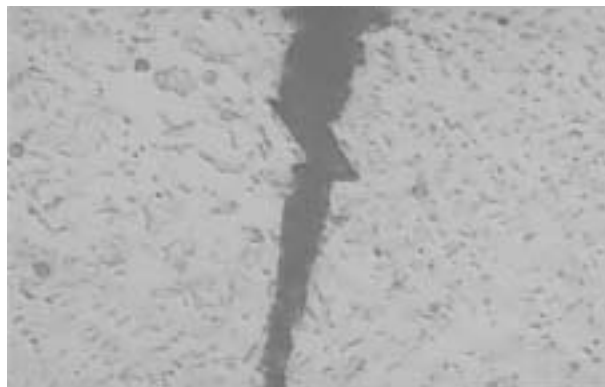


Figure 7. **Propagation of cleavage fracture over the M-A constituents, original magnification: 1000 \times , ($T_{p_2} = 980\text{ °C}$)**

Slika 7. **Širenje krtog loma preko M-A konstituenata, izvorno povećanje 1000 \times , ($T_{p_2} = 980\text{ °C}$)**

tion in the coarse-grained austenite was slower in compare with the γ - α phase transformation in the fine-grained austenite. Coarser-grained austenite has increased the tempering of weld metal. At the same time the probability of the formation of grain-boundary ferrite (GF) has reduced and the formation of acicular ferrite (AF) was enabled. The impact toughness of simulated microstructure of double-pass weld metal SM4 (Figure 8.) was a little lower in compare with the impact toughness of real single-pass weld metal SM1.

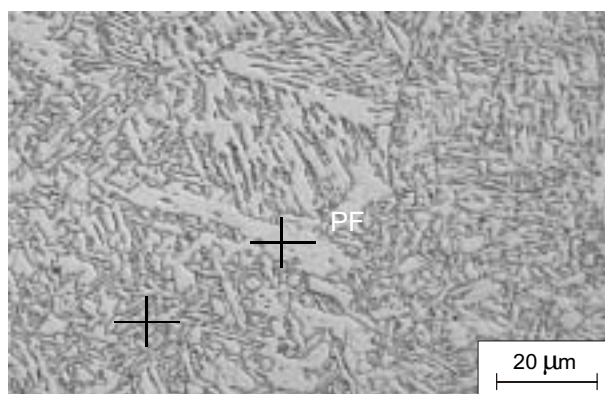


Figure 8. **Microstructure of polygonal ferrite (PF) and acicular ferrite (AF), ($T_{p_2} = 1100\text{ °C}$)**

Slika 8. **Mikrostruktura poligonalnog ferita (PF) i acikularnog ferita (AF), ($T_{p_2} = 1100\text{ °C}$)**

Relatively extend time of heating and cooling at simulated cycle $T_{p_2} = 1350\text{ °C}$ has enabled greater diffusion of carbon and alloying elements and the formation of homogenous austenite. High heating rate has hindered the solution of carbides in the first section of heating cycle. So,

the undissolved carbides were impeding the excessive growth of austenite grain. The α - γ phase transformation has not appeared above the equilibrium temperature T_0 , but the α -phase was superheated before the transformation has appeared. The α - γ phase transformation has extended. At the peak temperature $T_{p2} = 1350$ °C the carbides were completely dissolved. The simulated microstructure of double-pass weld metal SM5 (Figure 9.) was constituted from

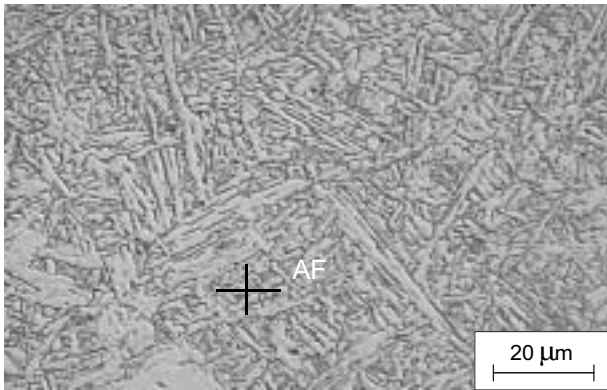


Figure 9. **Fine-grained acicular ferrite (AF), ($T_{p2} = 1350$ °C)**
Slika 9. **Finozrnati acikularni ferit (AF), ($T_{p2} = 1350$ °C)**

polygonal ferrite (PF) and acicular ferrite (AF). It has the greatest impact toughness in compare with the rests of the simulated microstructures. The impact toughness was almost identical with the impact toughness of real single-pass weld metal SM1 (Figure 3.).

CONCLUSIONS

The heating rate during the simulation of double-pass weld metal was very high. The α - γ phase transformation has not appeared above the equilibrium temperature, but the α -phase was partially superheated before the phase transformation has appeared. The high heating rate and the short holding time at the peak temperature have caused the formation of austenite with carbon inhomogeneities and residual carbides, and the limited grain growth in the intercritical and in the overcritical temperature region (up to 1100 °C). Superheating (short heating time) and presence of carbides have affected on the extent of the α - γ phase transformation. The dissolution of carbides (particularly cementite) occurs at temperature much greater than their expected solubility temperature, particularly with short heating times. The formation of homogenous austenite was shifted to the temperature region 1350 - 1400 °C.

At cooling from austenite region, the austenite has not transformed at exactly defined temperature, but the γ - α phase transformation was being occurring across the temperature interval. In the simulated microstructures of double-pass weld metal have formed the microstructures, which they otherwise significantly for different cooling rates. In

the intercritical temperature regions (between Ac_1 and Ac_3) and in the overcritical temperature regions (close by 980 °C) were appeared the M-A constituents. During the impact test, the M-A constituents have acted as cleavage fracture initiators. They have influenced rapidly on the decreasing the impact toughness of weld metal. The cooling times $\Delta t_{5/5} =$ between 12,6 s and 13,2 s have enabled only the partially transformation of the austenite into the bainite. Only a relatively extended times of heating and cooling (1350 °C) were enabled greater diffusion of carbon and alloying elements and formation of the homogenous austenite.

The results show, that the kinetics of transformation of austenite in the weld metal was slower in compare with the kinetics of transformation of austenite in the heat-affected zone. The weld metal was very stable and less sensitive for the thermal influence of the subsequent weld passes.

REFERENCES

- [1] F. Minami, M. Toyoda, K. Satoh: Effect of Mechanical Heterogeneity on Practical CTOD Evaluation of Welds, IIW Doc. X-1162-88, 1988.
- [2] S. H. Chung, H. Takahashi, M. Suzuki: Microstructural Gradient in HAZ its influence upon Toe HAZ Fracture Toughness, Japan, IIW Doc. X-861-77, 1977.
- [3] H. Satoh, M. Toyoda, Fracture Toughness Evaluation of Welds with Mechanical Heterogeneity, Transactions of the Japan Welding Society, 13 (1982) 1, 30 - 37.
- [4] F. Minami, M. Ohata, M. Toyoda, K. Arimochi, S. Suzuki, K. Bessyo, C. Thaulow, M. Hauge, Mis-Matching of Interfaces and Weld, GKSS Research Center Publications, Geesthacht, 1997, 319 - 330.
- [5] W. Soete: Embrittlement and Cracks in Steel Structures, Workshop on Pressure Vessels, Westinghouse Research Laboratory-Europe, Brussels, 1974.
- [6] K. Easterling, Introduction to the Physical Metallurgy of Welding, University of Lulea, Sweden, 1983, 105 - 155.
- [7] F. Matsuda, Y. Fukada, H. Okada, C. Shiga, K. Ikeuchi, Y. Horii, T. Shiwaku, S. Suzuki, Welding in the World, 37 (1996) 3, 134 - 154.
- [8] G. M. Evans, Welding Journal, 2 (1995), 249 - 261.
- [9] J. H. Tweed, J. F. Knott, Metal Science, 17 (1983), 45 - 54.
- [10] V. Gliha, Varilna tehnika, 42 (1993) 2, 56 - 60.
- [11] M. Nakanishi, N. Katsumoto, K. Kawai, H. Tsumura, Improvement of Toughness in Submerged Arc Metal of Thick Plates for Low Temperature Service, IIW Doc. IX-1414-86, 1986.
- [12] R. E. Dolby, Factors Controlling Haz and Weld Metal Toughness in C-Mn Steel, The welding Institute, Abington, Cambridge, England, 1979.
- [13] M. Toyosada, K. Nohara, T. Otsuka, Y. Hagiwara, Effect of Specimen Thickness and Local Brittle Zone on CTOD at HAZ of Weld Joint, IIW Doc. X-1104-86, 1986.
- [14] F. Minami, M. Toyoda, K. Satoh, Transactions of the Japan Welding Society, 19 (1988) 2, 1988, 45 - 53.
- [15] G. M. Evans, OERLIKON-Schweissmitteilungen, 49 (1991) 125, 22- 31.
- [16] Y. Sato, N. Hayakawa, T. Kuwana, Effect of Oxygen on Microstructure and Mechanical Properties of Steel Weld Metal, IIW Doc. IX-1742 - 94, 1994.
- [17] V. Gliha, Analiza nosilnosti homogenih večvarkovnih zvarnih spojev pri utrujanju z ozirom na vplive parametrov varjenja in gradnje vara, Univerza v Ljubljani, Naravoslovnotehniška fakulteta, doktorska disertacija, 1998.
- [18] D. Rojko, Izoblikovanje mikrostruktur večvarkovnega zvara s staljša termičnega vpliva varjenja, Univerza v Mariboru, Fakulteta za strojništvo, doktorska disertacija, 2003.